AAC Journals.ASM.org

Antiviral Effects of Artesunate on JC Polyomavirus Replication in COS-7 Cells

Biswa Nath Sharma,[a,b] Manfred Marschall,[c] Christine Hanssen Rinaldo[a,d]

Department of Microbiology and Infection Control, University Hospital of North Norway, Tromsø, Norway[a]; Department of Medical Biology, UiT The Arctic University of Norway, Tromsø, Norway[b]; Institute for Clinical and Molecular Virology, University of Erlangen-Nuremberg, Erlangen, Germany[c]; Metabolic and Renal Research Group, UiT The Arctic University of Norway, Tromsø, Norway[d]

The human JC polyomavirus (JCPyV) causes the fatal demyelinating disease progressive multifocal leukoencephalopathy (PML). A growing number of patients with induced or acquired immunosuppression are at risk for infection, and no effective antiviral therapy is presently available. The widely used antimalarial drug artesunate has shown broad antiviral activity *in vitro* but limited clinical success. The aim of this study was to investigate the effect of artesunate on JCPyV replication *in vitro*. The permissivity for JCPyV MAD-4 was first compared in four cell lines, and the monkey kidney cell line COS-7 was selected. Artesunate caused a concentration-dependent decrease in the extracellular JCPyV DNA load 96 h postinfection, with a 50% effective concentration (EC_{50}) of 2.9 μM. This effect correlated with a decreased expression of capsid protein VP1 and a reduced release of infectious viral progeny. For concentrations of <20 μM, transient reductions in cellular DNA replication and proliferation were seen, while for higher concentrations, some cytotoxicity was detected. A selective index of 16.6 was found when cytotoxicity was calculated based on cellular DNA replication in the mock-infected cells, but interestingly, cellular DNA replication in the JCPyV-infected cells was more strongly affected. In conclusion, artesunate is efficacious in inhibiting JCPyV replication at micromolar concentrations, which are achievable in plasma. The inhibition at EC_{50} probably reflects an effect on cellular proteins and involves transient cytostatic effects. Our results, together with the favorable distribution of the active metabolite dihydroartemisinin to the central nervous system, suggest a potential use for artesunate in patients with PML.

Progressive multifocal leukoencephalopathy (PML) is a rare and usually fatal demyelinating disease caused by the lytic replication of JC polyomavirus (JCPyV) in oligodendrocytes (1, 2). The disease mainly affects individuals afflicted with HIV-AIDS or patients undergoing treatment with certain immunomodulatory monoclonal antibodies, but it can also affect transplant patients and patients with hematological diseases or idiopathic CD4 T-cell lymphocytopenia (3–5). A few cases of PML in immunocompetent individuals have also been described (6, 7). Infrequently, JCPyV causes other diseases affecting the central nervous system (CNS) or kidneys (reviewed in reference 3). Infection with JCPyV is very common, and by adulthood, about 70% of all individuals are infected (8–10). After subclinical primary infection, JCPyV remains latent in the renourinary tract and possibly in the brain and lymphoid organs (11–14). Lifelong latency is interspersed by occasional asymptomatic reactivation, with shedding in urine (8, 9).

JCPyV belongs to the family *Polyomaviridae*, genus *Orthopolyomavirus* (15), and is a nonenveloped virus with an approximately 5-kb circular double-stranded DNA genome. The genome can be divided into 3 functional regions: the noncoding control region (NCCR), containing the origin of replication and promoters for early and late transcription, the early region, encoding the regulatory proteins small T antigen (sTag), large T antigen (LTag), and the derivates T′135, T′136, and T′165, and the late region, encoding the viral capsid proteins VP1, VP2, and VP3 and the agnoprotein, the function of which remains elusive (16). The NCCR of JCPyV found in the cerebrospinal fluid (CSF) or the brain of PML patients is typically rearranged, with deletions and insertions compared to that of the archetype virus shed in urine by healthy individuals. Interestingly, in cell culture, the rearranged viruses usually express higher levels of early gene products and exhibit a higher replication potential than the archetype virus (17).

Although human primary oligodendrocytes would be the most pathophysiologically relevant *in vitro* model for PML, these cells are difficult to obtain and propagate. Besides primary human fetal glial (PHFG) cells (1, 18) and human brain progenitor-derived astrocytes (PDA) (19), few human primary cell types are permissive for JCPyV (reviewed in reference 3). Most JCPyV studies have therefore been performed in simian virus 40 (SV40) immortalized cell lines expressing SV40 LTag, such as the African monkey kidney cell line COS-7 (20, 21), the human embryonic kidney cell line (HEK) 293TT (22, 23), which is probably of neuronal lineage (24), and the human fetal glial cell line SVG (25). These cell lines, though clearly different from primary oligodendrocytes, support rapid JCPyV replication, thus approximating the situation *in vivo*. Of note, the SVG p12 cell line from the ATCC was recently found to be contaminated with the closely related BK polyomavirus (BKPyV), but the frequently used subclone SVG-A may serve as a BKPyV-negative alternative (26).

Though a number of drugs have been explored *in vitro* and in a limited number of patients, no anti-JCPyV drug with proven efficacy is yet available (reviewed in reference 3). Artesunate is recommended by the WHO for the treatment of severe malaria, in

Received 26 June 2014 Returned for modification 22 July 2014
Accepted 20 August 2014
Published ahead of print 25 August 2014
Address correspondence to Christine Hanssen Rinaldo, christine.rinaldo@unn.no.

doi:10.1128/AAC.03714-14

particular with multidrug-resistant malaria (27), and has shown broad antiviral activity *in vitro* (28–33). Apparently, it has been successfully used to treat four transplant patients with recurrent multidrug-resistant cytomegalovirus (CMV) infection (34, 35) and one child with human herpesvirus 6 infection (36), but it did not give satisfactory results in other patients (35, 37, 38). Recently, we reported that artesunate has antiviral activity against BKPyV in human primary renal proximal tubular epithelial cells (RPTECs) and that the antiviral effect is connected to transient cytostatic effects without cytotoxicity (39). Encouraged by this and the good safety profile of artesunate, with a low incidence of side effects found in numerous studies (reviewed in reference 32), we investigated its effects on JCPyV replication. We started by comparing the permissivity for JCPyV MAD-4 in COS-7, HEK 293TT, SVG-A, and M03.13 cells, with M03.13 being an immortalized human-human hybrid cell line with the phenotypic characteristics of primary oligodendrocytes (40). Here, we demonstrate that COS-7 is the most suitable cell line for JCPyV MAD-4 antiviral studies and that artesunate inhibits the replication of JCPyV MAD-4 in COS-7 cells by a mechanism closely connected to its transient cytostatic effect.

MATERIALS AND METHODS

JCPyV MAD-4 propagation. The experiments were performed with JCPyV MAD-4 (strain ATCC VR-1583), a viral strain with a rearranged NCCR originally isolated from the brain of a PML patient (41) and previously used for antiviral studies (19).

The plasmid pGEMMAD-4, containing the complete JCPyV MAD-4 genome in a pGEM3Zf(+) vector (17), was kindly provided by Hans H. Hirsch, University of Basel, Switzerland. To generate infectious JCPyV MAD-4, the viral genome was prepared and transfected into COS-7 cells, as previously described (17). The supernatant was replaced by fresh medium at 7 days and 14 days posttransfection, and infectious virus was harvested by 6 cycles of freezing and thawing, followed by centrifugation at 900 rpm for 5 min to clarify the supernatants. To produce more virus, the first passage of JCPyV MAD-4 was used to infect new COS-7 cells. The medium was changed at 7 days postinfection (dpi). At 14 dpi, the supernatant containing JCPyV MAD-4 at a viral load of 2.14×10^{10} genomic equivalents (GEq)/ml was harvested, diluted in fresh medium to 7.1×10^{9} GEq/ml, and used for infection, as described below.

Cell propagation. HEK 293TT (22) was propagated in Dulbecco's modified Eagle's medium (DMEM) (catalog no. D5796; Sigma) with sodium pyruvate (100 mM) and 10% fetal bovine serum (FBS). SVG-A (25, 42), kindly provided by Walter Atwood, Brown University, RI, USA, was propagated in minimal essential medium (MEM) (catalog no. M4655; Sigma) with 10% FBS. M03.13 (CELLutions Biosystems, Inc.) (40) was propagated in DMEM (catalog no. D5796; Sigma) with 10% FBS, as instructed by the supplier, and COS-7 (strain ATCC RL1651) was propagated in DMEM (DMEM-H) (catalog no. D5671; Sigma) containing 1% GlutaMAX (equivalent to 2 mM L-glutamine) (Life Technologies) and either 10 or 3% FBS.

JCPyV MAD-4 permissivity study. HEK 293TT, SVG-A, COS-7, and M03.13 cells were propagated in their respective media supplemented with 10% FBS. One day before infection, 15,000 cells per 0.95 cm^2 well were seeded, and the next day, the approximately 60% confluent cells were infected with 100 μl of JCPyV MAD-4 supernatant for 2 h before surplus infectious units were removed; the cells were washed once with phosphate-buffered saline (PBS), and complete medium was added.

Infection and drug treatment. Artesunate (Saokim Pharmaceutical Co., Ltd., Hanoi, Vietnam) was dissolved in dimethyl sulfoxide (DMSO) to a concentration of 65 mM and immediately stored in aliquots at −70°C. Prior to use, the stock was diluted in DMEM with 3% FBS to working concentrations. One day before infection, 15,000 COS-7 cells per 0.95 cm^2 well were seeded in DMEM complete growth medium containing 3% FBS. The cells were infected with JCPyV MAD-4, as described above, before complete medium with or without increasing concentrations of artesunate was added. A DMSO control matching the DMSO concentration in 20 μM artesunate was included in all experiments.

Quantification of extracellular and intracellular JCPyV DNA loads. To quantify the extracellular JCPyV DNA loads, the cell culture supernatants were harvested and stored at −70°C until quantification by quantitative PCR (qPCR) using primers and a probe targeting the JCPyV LTag gene, as described elsewhere (43). Shortly before qPCR, the supernatants were diluted in distilled H_2O (1:100 dilution) and boiled for 5 min. To quantify the intracellular JCPyV DNA load, the DNA was first extracted from the cells using the MagAttract DNA mini M48 kit (Qiagen). In brief, the cells were washed once with PBS, lysed by adding buffer G2, and immediately stored at −70°C until robotic extraction (GenoM-48; Qiagen). The intracellular JCPyV DNA loads were quantified by qPCR as described for extracellular JCPyV loads but without dilution and boiling. Each experiment had duplicate samples measured in triplicate.

Immunofluorescence staining, microscopy, and digital image processing. The JCPyV MAD-4-infected cells with or without artesunate treatment were fixed at 96 h postinfection (hpi) in 4% paraformaldehyde (PFA) for 5 min and permeabilized by methanol for 10 min. Immunofluorescence staining was then performed using as primary antibodies a polyclonal rabbit antiserum directed against the C-terminal part of BKPyV LTag (1:1,000 dilution) (44) and a monoclonal mouse antiserum directed against JCPyV VP1 (1:400 dilution) (catalog no. ab34756; Abcam). As secondary antibodies, an anti-mouse antibody conjugated with Alexa Fluor 568 (1:500 dilution; Molecular Probes) and an anti-rabbit antibody conjugated with Alexa Fluor 488 (1:500 dilution; Molecular Probes) were used. The nuclei were labeled with Draq5 dye (1:1,000 dilution) (BioStatus). Images were collected using a Nikon TE2000 microscope (×10 objective) and processed with NIS-Elements BR 3.2 (Nikon Corporation).

Infectious progeny virus release. The supernatants harvested from untreated and artesunate-treated JCPyV MAD-4-infected COS-7 cells at 96 hpi for the determination of extracellular JCPyV DNA loads were diluted 1:2 and used to infect COS-7 cells. The infection was performed as described above, but this time, growth medium without artesunate was added. At 96 hpi, the cells were fixed, and immunofluorescence staining was performed as described above.

Cell proliferation and cell viability assays. The proliferation of mock-infected and JCPyV-infected COS-7 cells with or without artesunate treatment was monitored in real time by the xCELLigence system using a real-time cell analyzer (RTCA) dual-plate (DP) instrument, as previously described (45). This system measures the electrical impedance, which is influenced by adhesion, and the number and size of the cells, and this is expressed as an arbitrary unit (cell index) that reflects cell proliferation and viability. One day before infection, 6,000 cells per 0.2 cm^2 well were seeded in a volume of 200 μl. In order to avoid disturbances of the cell index, the supernatants were never completely removed from the wells. In short, 120 μl of supernatant was removed from each well, and 80 μl of the JCPyV infectious supernatant (undiluted) was added for 2 h before the infectious surplus was successively removed by a dilution method of 3 cycles. In each cycle, 150 μl of the supernatant was removed and replaced by 150 μl of fresh medium. At the end, 100 μl of the medium was left in all wells. Thereafter, 100 μl of medium with artesunate in double concentration or without artesunate was added. The mock-infected cells were treated the same way. The cell index was measured every 15 min for the first 6 h after seeding and every 30 min thereafter. In addition, the cell viability of the artesunate-treated COS-7 cells was measured by three different endpoint assays. In short, 6,000 cells per 0.32 cm^2 well were seeded, and the next day, the cells were either mock infected or JCPyV infected by incubation with 80 μl of the JCPyV infectious supernatant for 2 h. Next, the surplus infectious JCPyV was removed, and the cells were treated with increasing concentrations of artesunate. At 24, 48,

72, and 96 h posttreatment (hpt), cellular DNA replication was quantified by a colorimetric measurement of 20 h bromodeoxyuridine (BrdU) incorporated into DNA using the cell proliferation enzyme-linked immunosorbent assay (ELISA) and BrdU assay (Roche), and the total metabolic activity was monitored by the colorimetric measurement of 3 h of reduction of resazurin dye by mitochondrial, microsomal, and cytosolic enzymes using the TOX-8 assay (Sigma), as described earlier (39, 46). As an alternative measure of the total cellular metabolic activity, the ATP content of both the mock-infected and JCPyV-infected cells was measured at 96 hpt by the CellTiter-Glo luminescent cell viability assay (Promega), according to the manufacturer's instructions. In short, 100 μl of the CellTiter-Glo reagent was added to each well containing 100 μl of supernatant, and the plate was mixed for 2 min on a shaker to induce cell lysis. The plate was then incubated for 10 min at room temperature to stabilize the luminescent signal, and luminescence was measured using Tecan Infinite F200PRO reader (Tecan).

The cytotoxic effects of artesunate on the mock-infected or JCPyV-infected COS-7 cells were measured by the CellTox green cytotoxicity assay (Promega) at 24, 48, 72, and 96 hpt, as described by the manufacturer. The assay measures the changes in the membrane integrity of the cell using a green cyanine dye that is excluded from viable cells and preferentially stains the DNA from dead cells. When the dye binds DNA released from the cells, its fluorescence properties are substantially enhanced. According to the manufacturer, signals are stable for ≥3 days, and the same wells can be measured several times. Cell seeding, JCPyV infection, and artesunate treatment were carried out as described earlier, but this time, the green dye was included in artesunate at a 1:1,000 dilution. The fluorescence activity of the dye was measured at 24, 48, 72, and 96 hpt at an excitation/emission of 485/520 nm, with 5 flashes using a Tecan Infinite F200 PRO reader (Tecan).

Selectivity index of artesunate. The extracellular JCPyV load and cellular DNA replication at 96 hpi/hpt were analyzed by the XLfit program (fit model 205, dose-response one site, four-parameter logistic/sigmoidal dose response; IDBS Solutions) with fit equal to $A + [(B - A)/(1 + [C/x]^D)]$ to determine the effective concentration of artesunate giving a 50% inhibition of extracellular JCPyV DNA load (EC_{50}) and the 50% cytotoxic concentration (CC_{50}). The selectivity index (SI_{50}) was calculated by dividing the CC_{50} by the EC_{50}.

RESULTS

Comparison of replication efficiency of JCPyV MAD-4 in different cell lines. In order to find the most permissive cell line for our JCPyV antiviral study, the replication of JCPyV MAD-4 was investigated in COS-7, HEK 293TT, SVG-A, and M03.13 cells. First, extracellular and intracellular JCPyV DNAs were examined by qPCR at 1, 4, and 7 dpi. Comparing the extracellular JCPyV DNA load at 7 dpi to that at 1 dpi, which represents input JCPyV DNA, total increases of 0.9, 1.1, and 0.3 log JCPyV DNA were found in the supernatants from the COS-7, HEK 293TT, and SVG-A cells, respectively (Fig. 1A). At the same time, the intracellular JCPyV DNA loads increased by 1.5, 1.6, and 0.3 log, respectively (Fig. 1A). Of note, for both the COS-7 and HEK 293TT cells, an increase in the intracellular JCPyV DNA load was observed already at 4 dpi. However, for the M03.13 cells, there was no increase but rather a decrease in intracellular and extracellular JCPyV DNA at 4 and 7 dpi. Next, immunofluorescence staining was performed at 4 dpi using primary antibodies directed against JCPyV VP1 and BKPyV LTag. The BKPyV LTag antibody is known to cross-react with SV40 LTag and JCPyV LTag. VP1-expressing cells were found in the wells of the COS-7, HEK 293TT, and SVG-A cells (Fig. 1B, red), but the highest number was found in the wells with COS-7 cells. As expected, the COS-7, HEK 293TT, and SVG-A cells all constitutively expressed SV40 LTag (Fig. 1B, green), while no SV40 or JCPyV LTag expression was found in the M03.13 cells.

To investigate if the cellular origin of the virus played a role, the experiment was repeated with JCPyV MAD-4 generated in human SVG-A cells, but the results showed the same trend, suggesting that the cellular origin played no role (data not shown). We concluded that COS-7 and HEK 293TT cells are the most permissive of the tested cells for JCPyV MAD-4 infection and that M03.13 cells apparently are nonpermissive for at least this strain of JCPyV. Since we and others have experienced that HEK 293TT cells detach easily and therefore are not well suited for microscopic analysis or studies lasting several days (47), we decided to use COS-7 cells for all further experiments.

Artesunate inhibits JCPyV replication in COS-7. The one-step replication cycle of JCPyV in COS-7 cells grown in medium containing 2% FBS is known to be 4 days (21). In agreement with this, an approximately 1-log increase in extracellular JCPyV DNA load was found at 4 dpi when COS-7 cells were cultured in medium containing 3% FBS (data not shown) but not when 10% FBS was used (Fig. 1A). Therefore, we decided to use a 3% FBS concentration for all experiments. Comparing the extracellular JCPyV DNA load from the untreated cells at 96 hpi to that of 24 hpi (input), a 0.9-log increase was observed (Fig. 2A). The addition of 0.625 to 80 μM artesunate reduced the extracellular JCPyV DNA load in a concentration-dependent manner (Fig. 2A). While artesunate at 2.5, 10, and 20 μM reduced the JCPyV load by approximately 0.3 log (48%), 0.6 log (75%), and 0.8 log (84%), respectively, higher artesunate concentrations reduced JCPyV to the level of input virus. Of note, the DMSO control showed no inhibition of the JCPyV load.

Next, we investigated the effect of artesunate on JCPyV VP1 expression at 96 hpi by performing VP1 immunofluorescence staining. Compared to the untreated cells, a concentration-dependent reduction of VP1-expressing cells was detected (Fig. 2B, red). Of note, microscopy also revealed a slight reduction in cell numbers when 20 μM artesunate was used and a dramatic reduction when 40 and 80 μM artesunate were used (Fig. 2B, blue).

The supernatants harvested at 96 hpi were also tested for infectious progeny. The number of VP1-expressing cells was found to be inversely proportional to the original artesunate concentration (Fig. 2C, red), confirming a gradual reduction in the release of infectious progeny.

We conclude that artesunate inhibits JCPyV replication in COS-7 cells in a concentration-dependent manner.

Artesunate inhibits proliferation of mock-infected and JCPyV-infected COS-7 cells. Having observed a decreased cell number when artesunate concentrations of ≥20 μM were used, we investigated the influence of artesunate on cell viability in real time using the xCELLigence system. First, untreated mock-infected and JCPyV-infected COS-7 cells were compared by normalizing the cell index immediately after the addition of JCPyV. The cell index, which was slightly higher in JCPyV-infected than in mock-infected cells, was found to gradually increase up to ≥96 hpi, suggesting an increase in cell number, size of the cells, attachment, or a combination of these (Fig. 3A). Next, the effect of 1.25 to 40 μM artesunate was investigated, but this time, the cell index was normalized immediately after the addition of artesunate, and the cell index of the untreated cells was set as the baseline. A concentration-dependent decrease in the cell index of the artesunate-treated cells started from about 7 hpt (Fig. 3B and C). For mock-

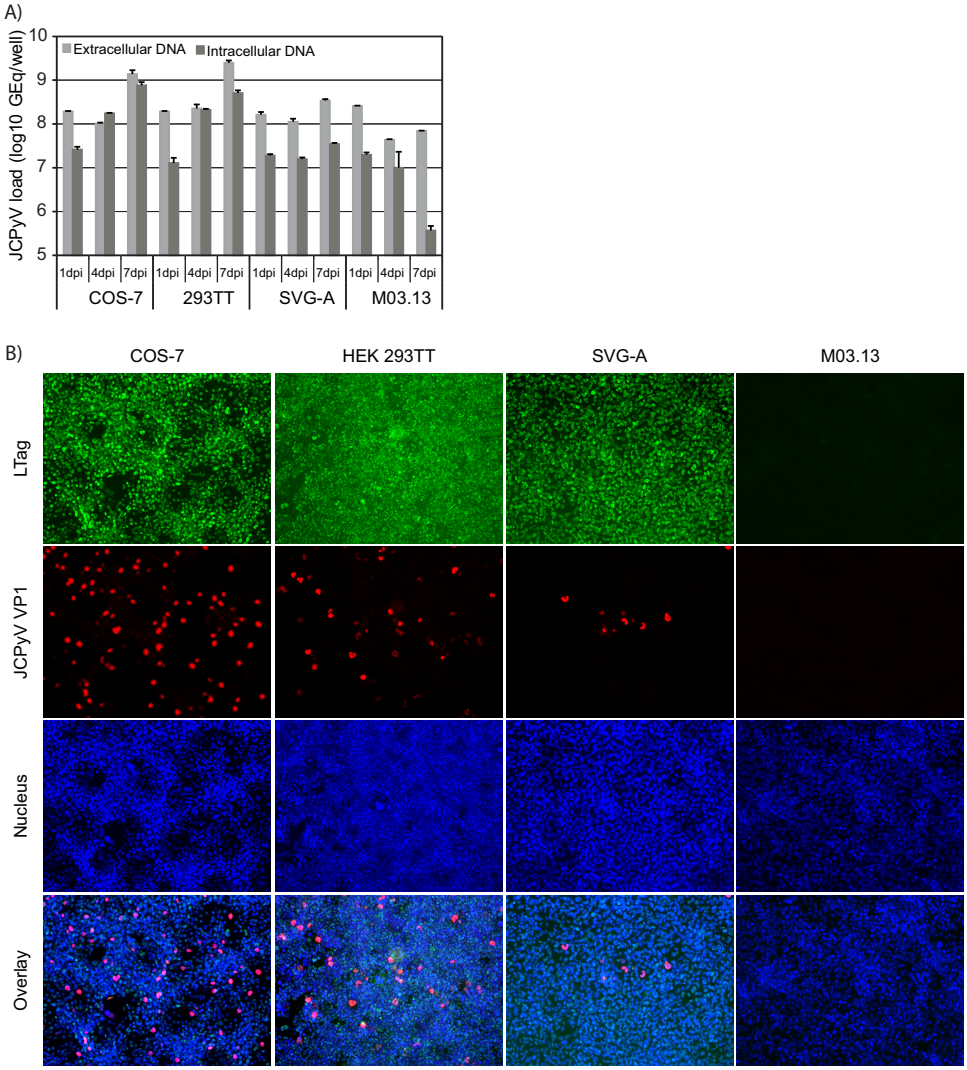

FIG 1 Permissivity of COS-7, HEK 293TT, SVG-A, and M03.13 cells for JCPyV MAD-4. The cells were infected with JCPyV MAD-4 for 2 h before the inoculum was replaced with fresh medium. (A) Extra- and intracellular JCPyV DNAs were quantified by qPCR of supernatants and extracted DNA from cell lysates, respectively, harvested at the indicated time points. The mean values (GEq/ml) ± standard deviations (SDs) of two parallel samples from one representative experiment are presented. (B) At 4 days postinfection, the cells were fixed and immunofluorescence staining performed using as primary antibody polyclonal rabbit anti-BKPyV LTag C-terminal serum that cross-reacts with SV40 LTag and JCPyV LTag (green) and a monoclonal mouse antibody directed against JCPyV VP1 (red). The cell nuclei (blue) were stained with Draq5. The pictures were taken with a fluorescence microscope (×10 objective).

infected cells treated with concentrations of <20 μM, the inhibition was completely reversed about 36 to 60 hpt, where the time to release correlated inversely with artesunate concentration (Fig. 3B). Interestingly, after the reversal of inhibition, the cells treated with 10 μM artesunate showed an increased cell index compared to that of the untreated cells. For cells treated with 20 and 40 μM artesunate, no reversal of inhibition was seen up to 96 h of treatment (Fig. 3B), but for the 20 μM concentration, the inhibition was reversed from 125 hpt (data not shown). The results from the JCPyV-infected cells were similar (Fig. 3C). To summarize our results from the xCELLigence system, artesunate was found to have a rapid and strong antiproliferative effect on both mock-infected and JCPyV-infected COS-7 cells, but the effect is transient for concentrations of <20 μM.

We next examined the effects of artesunate on cellular DNA replication and total metabolic activity in mock-infected cells by the use of BrdU and resazurin assays at 24, 48, 72, and 96 hpt. At 24 hpt, the DNA replication was reduced in a concentration-dependent manner (Fig. 4A). The largest reductions were found for 40 and 80 μM artesunate, which reduced DNA replication by 16 and 23%, respectively. For these two concentrations, further reductions of >40 and 70%, respectively, were observed at later time points. In contrast to this, for concentrations of <40 μM, the strongest inhibition of DNA replication was observed at 24 hpt. The inhibition gradually decreased at 48 and 72 hpt and was completely diminished at 96 hpt. In fact, at 96 hpt, DNA replication was higher in the artesunate-treated wells than in the untreated wells. At 24 hpt, the metabolic activity was also reduced in a concentration-dependent manner (Fig. 4B). The largest reductions were found for 40 and 80 μM artesunate, which reduced the metabolic activity by 37 and 58%, respectively. For these two concentrations, a further decrease was observed at 48 hpt, leading to total

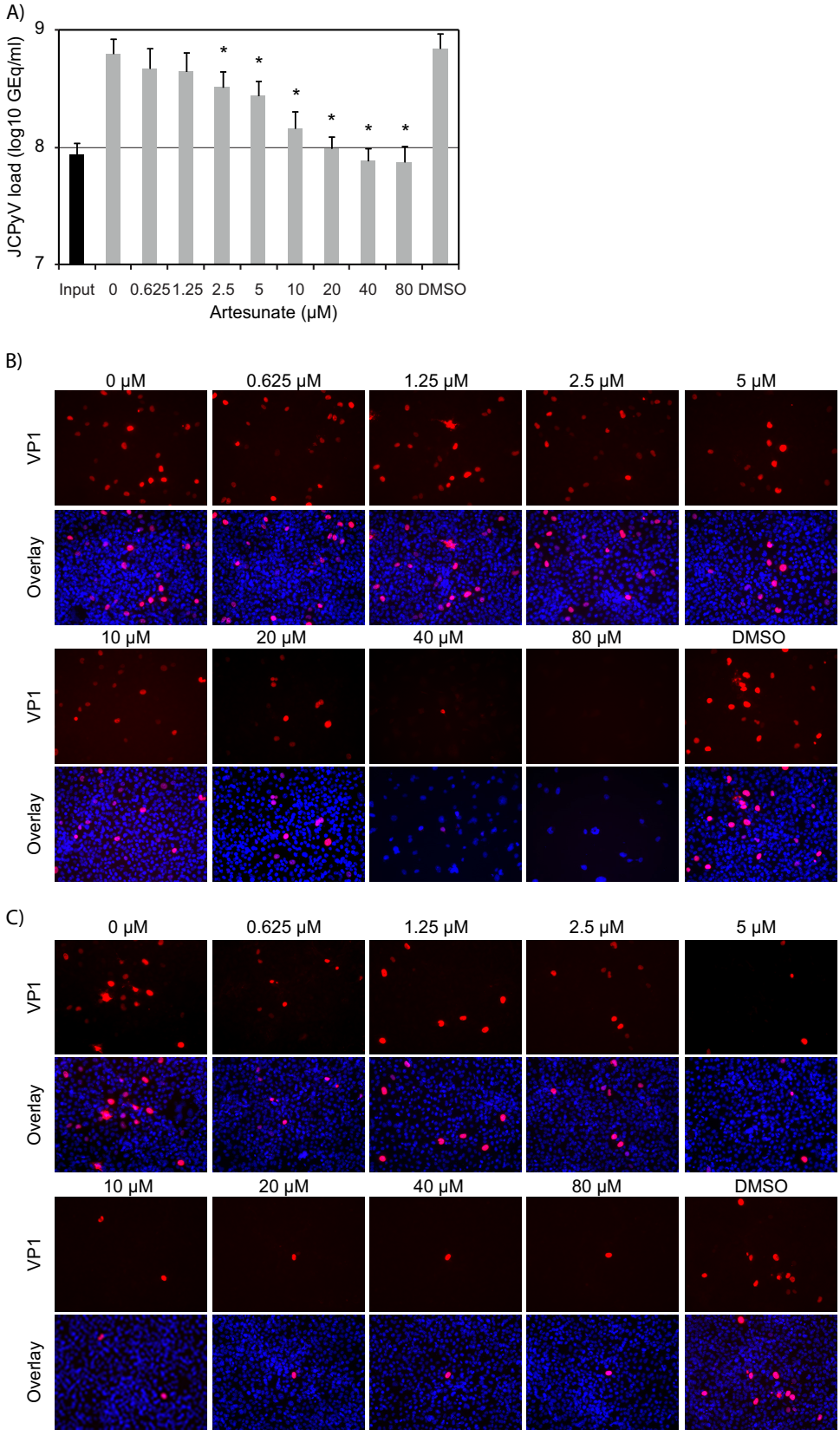

FIG 2 Effect of artesunate on JCPyV replication in COS-7 cells. (A) Extracellular JCPyV DNA load. At 96 hpi, supernatants were harvested from JCPyV-infected COS-7 cells treated with artesunate at the indicated concentrations, and the JCPyV DNA loads were measured by qPCR. In addition, supernatants harvested at 24 hpi were analyzed to obtain an input viral load. The mean values (GEq/ml) ± SDs from three independent experiments (each experiment had two parallel

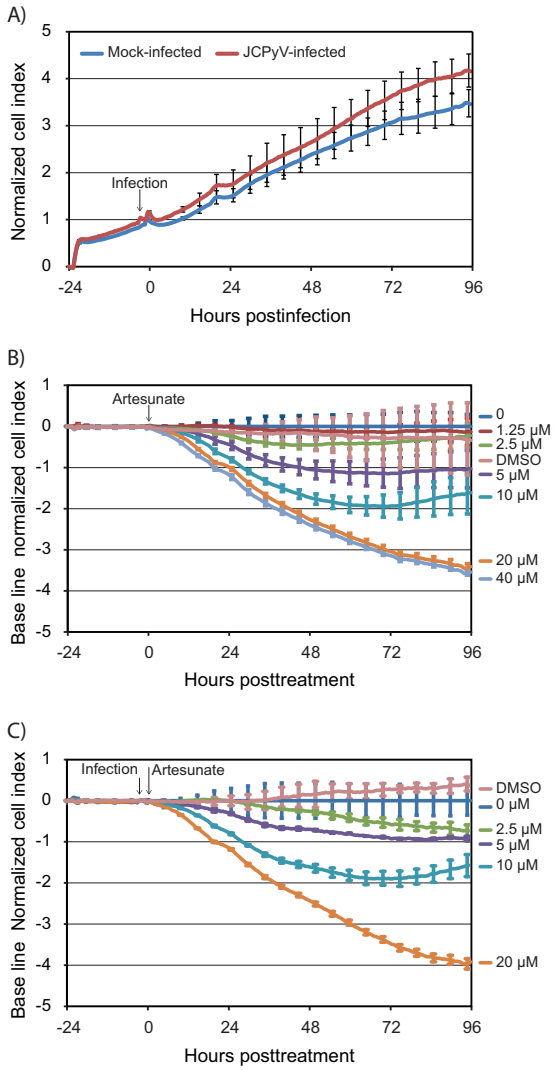

FIG 3 Effect of artesunate on cell proliferation of mock-infected and JCPyV-infected COS-7 cells in real time. The cells were monitored from the time of seeding up to 96 hpi (A) or 96 hpt (B and C) by an xCELLigence RTCA DP instrument, and the adhesion, together with the number and the size of the cells, was expressed as a cell index. Approximately 24 h after seeding, the cells were infected with conditioned medium or JCPyV for 2 h before the infectious inoculum was removed and replaced by growth medium with or without artesunate at the indicated concentrations (for details, see Materials and Methods). (A) The cell index of mock-infected and JCPyV-infected cells was normalized immediately after infection. The cell index of the untreated and artesunate-treated mock-infected cells (B) and JCPyV-infected cells (C). (B and C) The cell index was normalized immediately after treatment, and the cell index of the untreated cells was set as baseline 0. The mean values ± SDs of 3 to 4 wells (mock infected) and of 2 wells (JCPyV infected) from one representative experiment out of three are shown.

reductions of about 75 and 90%, respectively. However, no further reduction was seen over the next 2 days. In contrast to this, the inhibition of metabolic activity caused by artesunate concentrations of <40 μM was not significantly changed over the next 3 days.

To investigate if the cellular DNA replication and metabolic activity of JCPyV-infected cells were similarly affected, BrdU and resazurin assays were also performed in the infected cells at 96 hpt (98 hpi), and the results were normalized to untreated mock-infected cells. A concentration-dependent reduction of the DNA replication was found (Fig. 4C), and at all concentrations of >5 μM, DNA replication was significantly more affected than that in the mock-infected cells (Fig. 4A). The metabolic activity, which was slightly higher in JCPyV-infected than in mock-infected cells, was reduced in a concentration-dependent manner (Fig. 4D), similar to in the mock-infected cells (Fig. 4B).

In order to verify the metabolic activity results, the CellTiter-Glo assay was used at 96 hpt (98 hpi). Similar to the results obtained by the resazurin assay and by intracellular lactate dehydrogenase (LDH) assay (39) (data not shown), the total metabolic activity (ATP content) was found to decrease with increasing artesunate concentrations (Fig. 4E). Furthermore, the ATP content, reflecting the number of viable cells, was less in the JCPyV-infected wells than in the mock-infected wells. The difference was the most pronounced in the untreated cells, suggesting that artesunate prevented lytic JCPyV replication.

In order to investigate the potential cytotoxic effects of artesunate, the CellTox green cytotoxicity assay was performed at 24, 48, 72, and 96 hpt. At 24 hpt, no significant increase in cell death was found for any artesunate concentration in either the mock-infected (Fig. 5A) or JCPyV-infected cells (Fig. 5B). However, from 48 hpt, concentrations of >10 μM resulted in increased cell death in both the mock-infected and JCPyV-infected cells. For the JCPyV-infected cells, the results were confirmed by the use of the cytotoxicity LDH assay (data not shown).

When the results from all cell viability assays are taken together, they suggest that the addition of artesunate quickly slowed down or completely stopped cell proliferation in a concentration-dependent manner. DNA replication and metabolic activity were reduced as early as 24 hpt. However, for artesunate concentrations up to 10 μM, no significant cytotoxicity was observed, and the inhibition was transient and followed by an increase in the DNA replication and proliferation compared to those of the untreated cells. Since the DMSO control did not have significant effects on cell viability, all observed effects were assumed to be caused by artesunate and not the solvent.

We conclude that the antiproliferative effect of artesunate on mock-infected and JCPyV-infected COS-7 cells is mainly due to cytostatic effects for concentrations up to and including 10 μM and is due to a combination of cytostatic and cytotoxic effects at higher concentrations. Moreover, the infected cells seem to be more sensitive to cytostatic effects than the mock-infected cells.

samples) are presented. *, $P < 0.05$, determined by the *t* test. (B) Expression of JCPyV late protein. At 96 hpi, JCPyV-infected COS-7 cells treated with the indicated concentrations of artesunate from 2 hpi were fixed and immunofluorescence staining performed with the monoclonal mouse anti-JCPyV VP1 antibody to visualize JCPyV late protein VP1 (red) and with Draq5 to visualize the nuclei (blue). The pictures were taken with a fluorescence microscope (×10 objective). (C) Infectious progeny release. The supernatants from untreated and artesunate-treated JCPyV-infected COS-7 cells harvested at 96 hpi were diluted 1:2 in medium and seeded onto new COS-7 cells. At 96 hpi, the cells were fixed and immunostained as described for panel B. The pictures were taken with a fluorescence microscope (×10 objective).

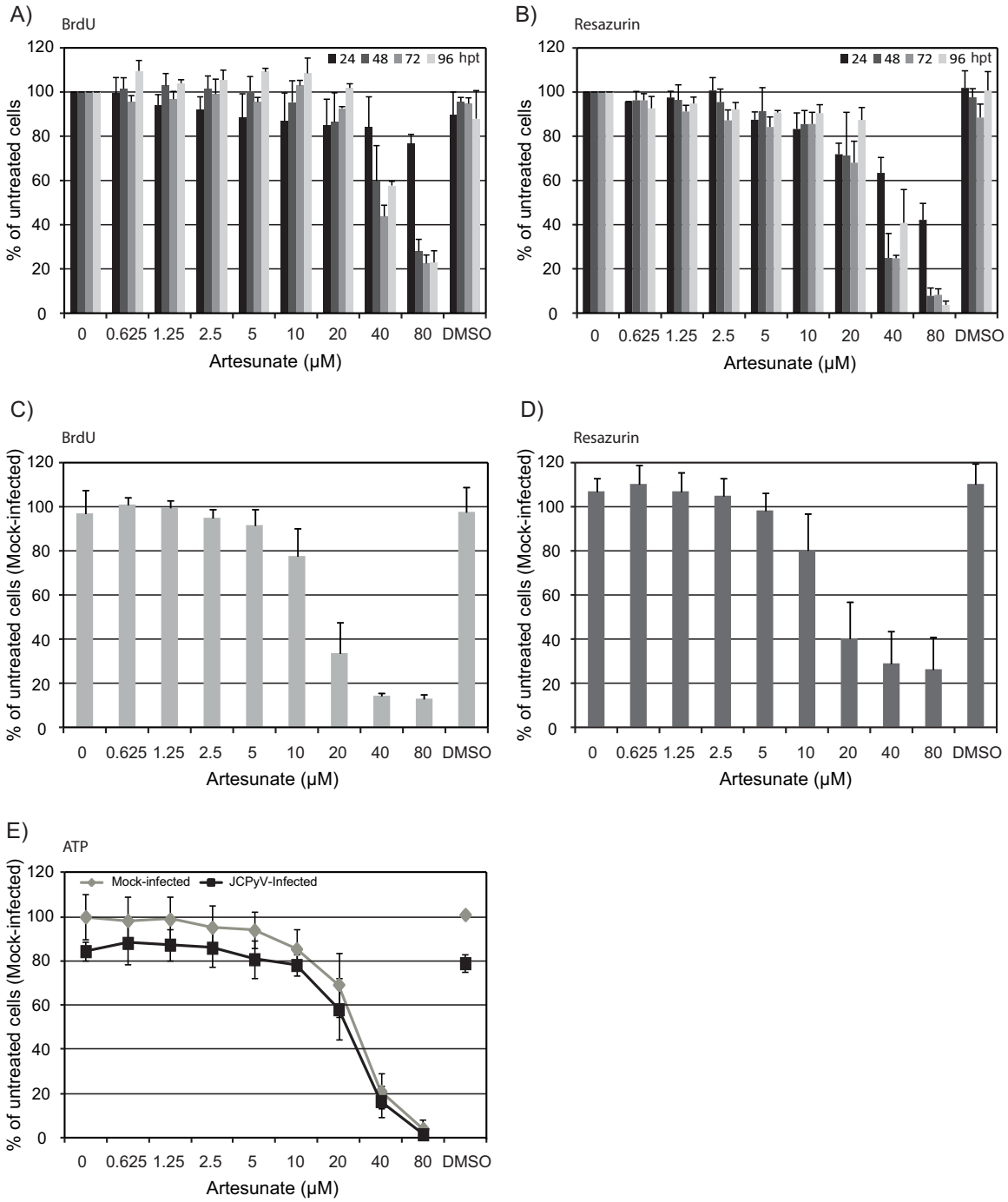

FIG 4 Cell viability of artesunate-treated mock-infected and JCPyV-infected COS-7 cells. The cellular DNA replication (A) and total metabolic activity (B) of mock-infected COS-7 cells were measured at 24, 48, 72, and 96 hpt. The cellular DNA replication (C) and total metabolic activity (D) of JCPyV-infected COS-7 cells were measured at 96 hpt (98 hpi). (E) The ATP content of metabolically active mock-infected and JCPyV-infected COS-7 cells was measured at 96 hpt (98 hpi) (for details, see Materials and Methods). The mean values ± SDs from two to three experiments are presented as the percentage of untreated cells. Each experiment was performed in 3 parallel wells.

Determination of the selective index of artesunate in COS-7 cells. An EC_{50} (±95% confidence interval [CI]) of 2.9 ± 0.7 μM ($P < 0.001$) was calculated based on the data in Fig. 2A (Fig. 6). Since very little toxicity was observed in the artesunate-treated cells, a CC_{50} (±95% CI) of 48.2 ± 12.0 μM ($P < 0.001$) was calculated based on cellular DNA replication of mock-infected cells at 96 hpt (Fig. 4A), as previously described (39, 45, 46) (Fig. 6). This gave an SI_{50} (CC_{50}/EC_{50}) of 16.6. When the CC_{50} (±95% CI) was calculated based on cellular DNA replication of the JCPyV-infected cells, this was found to be 19.2 ± 4.5 μM ($P < 0.001$) (Fig. 6), giving an SI_{50} of 6.6, indicating a stronger effect on the JCPyV-infected than the mock-infected cells. By extrapolating

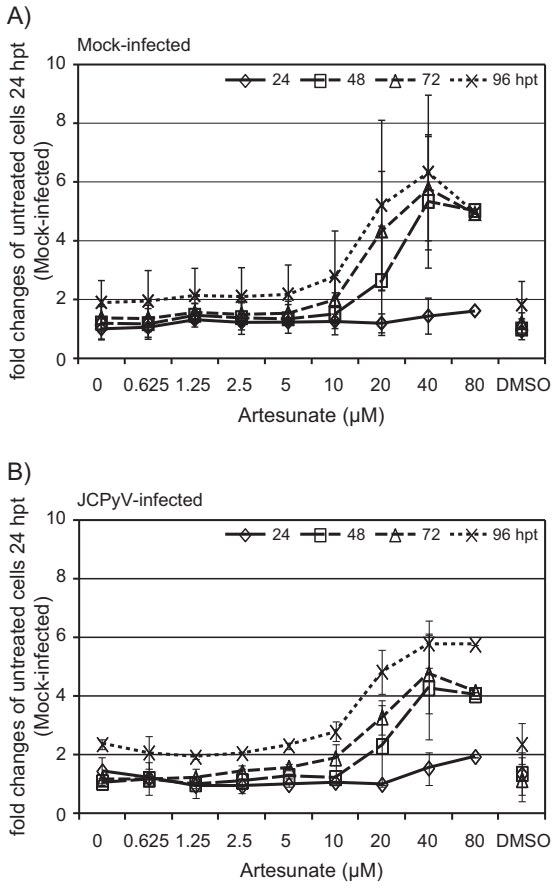

FIG 5 Cytotoxicity of artesunate-treated mock-infected and JCPyV-infected COS-7 cells. Mock-infected (A) and JCPyV-infected (B) COS-7 cells were treated with the indicated concentrations of artesunate containing the CellTox green dye from 2 hpi. This dye has increased fluorescence intensity when bound to the DNA of cells with an impaired cell membrane. The fluorescence intensity of the dye was measured at 24, 48, 72, and 96 hpt. To correlate the cell death found in artesunate-treated cells with that in the untreated cells, the fluorescence intensity of each drug concentration measured at all time points was divided by that of untreated mock-infected cells at 24 hpt. The mean values ± SDs from two individual experiments are presented as fold changes, and each experiment was performed in 3 parallel wells.

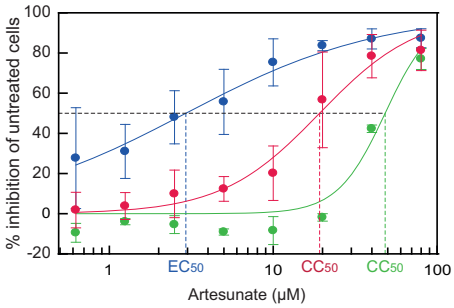

FIG 6 Determination of artesunate EC_{50} and CC_{50} by curve fitting. To determine the EC_{50} (blue, JCPyV load) and CC_{50} (red, JCPyV-infected cells, and green, mock-infected cells), the effect of increasing concentrations of artesunate on extracellular JCPyV DNA loads and on cellular DNA replication (BrdU incorporation) was analyzed by curve fitting using the XLfit program. The mean values ± SDs from three experiments are presented.

from the dose-response curve (Fig. 6), an EC_{90} (± 95% CI) of 57.7 ± 34.7 μM ($P = 0.458$) was estimated, which suggested that 90% of inhibition was dependent on cytotoxic effects.

We conclude that artesunate treatment of JCPyV-infected COS-7 cells has an SI_{50} of 16.6 when CC_{50} was calculated using mock-infected cells but only 6.6 when CC_{50} was calculated using JCPyV-infected cells.

DISCUSSION

An effective antiviral drug is urgently needed to treat patients with PML. Since the antimalarial drug artesunate has shown broad antiviral effects, we explored its antiviral activity on JCPyV replication in permissive COS-7 cells. The data presented here indicate that artesunate inhibits JCPyV replication in COS-7 cells and that this is connected to a transient cytostatic effect. Artesunate reduced the extracellular JCPyV DNA load and infectious progeny release at 96 hpi in a concentration-dependent manner, with an EC_{50} of 2.9 μM. Artesunate concentrations of ≥2.5 μM clearly reduced the number of cells expressing VP1, while the total cell numbers were decreased at concentrations of ≥20 μM. The cell index measurements revealed a rapid concentration-dependent inhibition of cell proliferation in both the mock-infected and JCPyV-infected cells, but for all concentrations of <20 μM, the inhibition was only transient. In agreement with this, cellular DNA replication in mock-infected cells was most strongly affected at 24 hpt and reverted to normal or even higher levels at 96 hpt, at least for concentrations of <40 μM. Of note, this was different for JCPyV-infected cells, for which the DNA replication was still reduced at 96 hpt. Only concentrations of ≥20 μM caused increased cell death in the mock-infected and JCPyV-infected cells, and an SI_{50} of 16.6 was found when cellular DNA replication was used to calculate the CC_{50} of the mock-infected cells.

Unfortunately, primary oligodendrocytes, which are the major target cells in PML, could not be obtained for this study. Although astrocytes may be infected by JCPyV in PML, the infection is rarely productive (3, 48), perhaps because the cells instead engage in removing infected oligodendrocytes (49). In our experience, primary human astrocytes are also poorly permissive for JCPyV (S. Henriksen, unpublished data) and would not provide sufficient analytic strength to accurately quantify antiviral effects. COS-7 cells were therefore chosen. Of note, the enhanced replicative ability of the PML-derived rearranged JCPyV strain MAD-4 probably played only a minor role due to the constitutive expression of SV40 LTag in these cells (17).

With regard to JCPyV replication, artesunate caused a concentration-dependent reduction in the extracellular JCPyV DNA load. Similar to the 65% reduction of the extracellular BKPyV load found in RPTECs (39), 10 μM artesunate reduced the extracellular JCPyV DNA load by 75%, and this correlated with a decrease in the number of VP1-expressing cells and in infectious progeny release. The EC_{50} of 2.9 μM was in the same range as that found for BKPyV (4.2 μM) (39) and for herpesviruses (2.16 to 7.21 μM) (29, 31, 50–52), although different host cells were used. Artesunate affects a very early stage of herpesvirus infection, but the mechanism seems to be the inhibition of cellular pathways (50). In BKPyV-infected RPTECs, artesunate inhibited early gene expression but also viral DNA replication, late gene expression, and the release of progeny virus (39). Since COS-7 cells constitutively express SV40 LTag, which can initiate viral DNA replication from the JCPyV origin (53), and no specific antibody for JCPyV LTag

was available, the effects on early protein expression and of the later connected steps in the replication cycle were not investigated.

With regard to cell viability, artesunate concentrations of ≥20 μM visibly reduced the cell numbers. In agreement with this, real-time cell analysis demonstrated a rapid concentration-dependent reduction of the cell index, but this was transient for concentrations of <20 μM. Moreover, the inhibitory effect on cellular DNA replication in the mock-infected cells was strongest at 24 hpt and then declined, except when 40 and 80 μM were used. The transient effect of artesunate is probably explained by a relatively short half-life in cell culture of about 12.4 h (52). Interestingly, the effect on total metabolic activity was not reversed up to 96 hpt. The explanation for this apparent discrepancy is probably linked to a cell cycle arrest in G_0 or G_2, as previously demonstrated in other cells (39, 54–56). When the effect of artesunate waned, a high proportion of the synchronized cells moved into the S phase and incorporated BrdU in their DNA, whereas the metabolic activity was still reduced due to reduced cell numbers. However, concentrations of >20 μM permanently inhibited DNA replication, probably reflecting a disability in reentering the cell cycle.

Interestingly, the cellular DNA replication was more affected in the JCPyV-infected cells than in the mock-infected cells at 96 hpt, especially when concentrations of ≥10 μM were used. The result is the opposite of that found in the BKPyV study in RPTECs (39) and is surprising, since all COS-7 cells express high levels of SV40 LTag, the key protein for stimulating entry into the S phase during infection (57). Based on the ATP levels, a slightly lower cell number was seen in the JCPyV-infected than in the mock-infected wells, but the difference was most pronounced in the untreated wells (15%) and therefore did not explain the difference found in regarding DNA replication. That the difference in cell numbers was not seen with the resazurin assay may be explained by an upregulation of the enzymes involved in the reduction of resazurin in the infected cells (Fig. 4D, untreated cells), similar to what has been reported for stressed amoebas (58). Only concentrations of ≥20 μM caused measurable cytotoxic effects. It should be mentioned that neurotoxicity has been observed exclusively in animal studies with high artesunate concentrations and never in humans given the recommended doses (59).

We have shown that artesunate inhibits the replication of JCPyV in COS-7 cells with an EC_{50} of 2.9 μM, a concentration that can be achieved in plasma (60–62). However, to be eligible for therapeutic treatment for PML, artesunate also needs to cross the blood-brain barrier and enter the CNS. In one study of six severely sick *Plasmodium falciparum*-infected patients treated with intravenous artesunate (approximately 2.3 mg/kg of body weight), artesunate was not detectable in CSF samples collected from 15 min to 120 min after injection but only in plasma collected at 15 min (63). However, dihydroartemisinin was found in plasma and CSF samples collected at all time points. Since the concentration in CSF increased over time while the concentration in plasma decreased over time, this suggests that dihydroartemisinin can enter and accumulate in the CSF (63). Although dihydroartemisinin has a favorable low molecular mass (284 Da) and is highly lipid soluble (64), it is not clear if it will reach and enter the affected oligodendrocytes.

Our results indicate that the anti-JCPyV activity of artesunate is based on the inhibition of virus-supportive cellular pathways rather than inhibition of a viral target, and this is compatible with the mechanism postulated for the broad antiherpesviral activity of artesunate (29, 32, 50). Importantly, the SI_{50}s of 16.6 and 6.6 from mock-infected and JCPyV-infected cells, respectively, suggest some specificity for JCPyV-infected COS-7 cells. One important question is how glial and neuronal cells will respond to artesunate. There is one study with the human astrocytoma line U373MG (65). Here, no cytotoxicity was observed at 96 hpt when artesunate concentrations of <50 μM were used, thereby suggesting a response similar to that seen in COS-7 cells. For PML, longer treatment courses than the 4 days used in our study or the usual 7-day regime for malaria (66) may be required. This seems feasible, since two transplant patients with multidrug-resistant CMV received artesunate for 4 and 7 months without adverse effects, although a third patient had to quit treatment after 1 month due to adverse gastrointestinal effects (35).

In conclusion, artesunate inhibits the replication of JCPyV in COS-7 cells, and the antiviral effect appears to be closely related to transient cytostatic effects. True cytotoxic effects were exclusively seen at artesunate concentrations of ≥20 μM, underlining the anti-JCPyV specificity in the low micromolar range. Since the EC_{50} of 2.9 μM can be achieved in human plasma and the active metabolite dihydroartemisinin accumulates in CSF, artesunate may prove to be useful for treating PML. In the near future, carefully designed clinical studies will have to address the pharmacokinetic details of the drug (e.g., penetration into the brain) and the effects of long-term treatment.

ACKNOWLEDGMENTS

We thank Garth D. Tylden at the Department of Microbiology and Infection Control of the University Hospital of North Norway for critical reading of the manuscript and helpful comments and Stian Henriksen of the same department for his excellent technical support and helpful comments.

The project is financially supported by the Northern Norway Regional Health Authority Medical Research Program. M.M. is supported by grants from the Deutsche Forschungsgemeinschaft (MA 1289/7-1 and MA 1289/7-2) and Wilhelm Sander-Stiftung (2011.085.1 and 2011.085.2).

REFERENCES

1. **Padgett BL, Walker DL, ZuRhein GM, Eckroade RJ, Dessel BH.** 1971. Cultivation of papova-like virus from human brain with progressive multifocal leucoencephalopathy. Lancet **i:**1257–1260.
2. **Ferenczy MW, Marshall LJ, Nelson CD, Atwood WJ, Nath A, Khalili K, Major EO.** 2012. Molecular biology, epidemiology, and pathogenesis of progressive multifocal leukoencephalopathy, the JC virus-induced demyelinating disease of the human brain. Clin. Microbiol. Rev. **25:**471–506. http://dx.doi.org/10.1128/CMR.05031-11.
3. **Hirsch HH, Kardas P, Kranz D, Leboeuf C.** 2013. The human JC polyomavirus (JCPyV): virological background and clinical implications. APMIS **121:**685–727. http://dx.doi.org/10.1111/apm.12128.
4. **Alstadhaug KB, Croughs T, Henriksen S, Leboeuf C, Sereti I, Hirsch HH, Rinaldo CH.** 2014. Treatment of progressive multifocal leukoencephalopathy with interleukin 7. JAMA Neurol. **71:**1030–1035. http://dx.doi.org/10.1001/jamaneurol.2014.825.
5. **Gheuens S, Wüthrich C, Koralnik IJ.** 2013. Progressive multifocal leukoencephalopathy: why gray and white matter. Annu. Rev. Pathol. **8:**189–215. http://dx.doi.org/10.1146/annurev-pathol-020712-164018.
6. **Naess H, Glad S, Storstein A, Rinaldo CH, Mørk SJ, Myhr KM, Hirsch H.** 2010. Progressive multifocal leucoencephalopathy in an immunocompetent patient with favourable outcome. A case report. BMC Neurol. **10:**32. http://dx.doi.org/10.1186/1471-2377-10-32.
7. **Gheuens S, Pierone G, Peeters P, Koralnik IJ.** 2010. Progressive multifocal leukoencephalopathy in individuals with minimal or occult immunosuppression. J. Neurol. Neurosurg. Psychiatry **81:**247–254. http://dx.doi.org/10.1136/jnnp.2009.187666.
8. **Egli A, Infanti L, Dumoulin A, Buser A, Samaridis J, Stebler C, Gosert**

R, Hirsch HH. 2009. Prevalence of polyomavirus BK and JC infection and replication in 400 healthy blood donors. J. Infect. Dis. **199:**837–846. http://dx.doi.org/10.1086/597126.

9. **Knowles WA, Pipkin P, Andrews N, Vyse A, Minor P, Brown DW, Miller E.** 2003. Population-based study of antibody to the human polyomaviruses BKV and JCV and the simian polyomavirus SV40. J. Med. Virol. **71:**115–123. http://dx.doi.org/10.1002/jmv.10450.
10. **Stolt A, Sasnauskas K, Koskela P, Lehtinen M, Dillner J.** 2003. Seroepidemiology of the human polyomaviruses. J. Gen. Virol. **84:**1499–1504. http://dx.doi.org/10.1099/vir.0.18842-0.
11. **Chesters PM, Heritage J, McCance DJ.** 1983. Persistence of DNA sequences of BK virus and JC virus in normal human tissues and in diseased tissues. J. Infect. Dis. **147:**676–684. http://dx.doi.org/10.1093/infdis/147.4.676.
12. **Monaco MC, Atwood WJ, Gravell M, Tornatore CS, Major EO.** 1996. JC virus infection of hematopoietic progenitor cells, primary B lymphocytes, and tonsillar stromal cells: implications for viral latency. J. Virol. **70:**7004–7012.
13. **White FA, III, Ishaq M, Stoner GL, Frisque RJ.** 1992. JC virus DNA is present in many human brain samples from patients without progressive multifocal leukoencephalopathy. J. Virol. **66:**5726–5734.
14. **Bayliss J, Karasoulos T, McLean CA.** 2012. Frequency and large T (LT) sequence of JC polyomavirus DNA in oligodendrocytes, astrocytes and granular cells in non-PML brain. Brain Pathol. **22:**329–336. http://dx.doi.org/10.1111/j.1750-3639.2011.00538.x.
15. **Johne R, Buck CB, Allander T, Atwood WJ, Garcea RL, Imperiale MJ, Major EO, Ramqvist T, Norkin LC.** 2011. Taxonomical developments in the family *Polyomaviridae*. Arch. Virol. **156:**1627–1634. http://dx.doi.org/10.1007/s00705-011-1008-x.
16. **Trowbridge PW, Frisque RJ.** 1995. Identification of three new JC virus proteins generated by alternative splicing of the early viral mRNA. J. Neurovirol. **1:**195–206. http://dx.doi.org/10.3109/13550289509113966.
17. **Gosert R, Kardas P, Major EO, Hirsch HH.** 2010. Rearranged JC virus noncoding control regions found in progressive multifocal leukoencephalopathy patient samples increase virus early gene expression and replication rate. J. Virol. **84:**10448–10456. http://dx.doi.org/10.1128/JVI.00614-10.
18. **Padgett BL, Rogers CM, Walker DL.** 1977. JC virus, a human polyomavirus associated with progressive multifocal leukoencephalopathy: additional biological characteristics and antigenic relationships. Infect. Immun. **15:**656–662.
19. **Gosert R, Rinaldo CH, Wernli M, Major EO, Hirsch HH.** 2011. CMX001 (1-*O*-hexadecyloxypropyl-cidofovir) inhibits polyomavirus JC replication in human brain progenitor-derived astrocytes. Antimicrob. Agents Chemother. **55:**2129–2136. http://dx.doi.org/10.1128/AAC.00046-11.
20. **Gluzman Y.** 1981. SV40-transformed simian cells support the replication of early SV40 mutants. Cell **23:**175–182. http://dx.doi.org/10.1016/0092-8674(81)90282-8.
21. **Hara K, Sugimoto C, Kitamura T, Aoki N, Taguchi F, Yogo Y.** 1998. Archetype JC virus efficiently replicates in COS-7 cells, simian cells constitutively expressing simian virus 40 T antigen. J. Virol. **72:**5335–5342.
22. **Buck CB, Pastrana DV, Lowy DR, Schiller JT.** 2004. Efficient intracellular assembly of papillomaviral vectors. J. Virol. **78:**751–757. http://dx.doi.org/10.1128/JVI.78.2.751-757.2004.
23. **Broekema NM, Imperiale MJ.** 2012. Efficient propagation of archetype BK and JC polyomaviruses. Virology **422:**235–241. http://dx.doi.org/10.1016/j.virol.2011.10.026.
24. **Shaw G, Morse S, Ararat M, Graham FL.** 2002. Preferential transformation of human neuronal cells by human adenoviruses and the origin of HEK 293 cells. FASEB J. **16:**869–871. http://dx.doi.org/10.1096/fj.01-0995fje.
25. **Major EO, Miller AE, Mourrain P, Traub RG, de Widt E, Sever J.** 1985. Establishment of a line of human fetal glial cells that supports JC virus multiplication. Proc. Natl. Acad. Sci. U. S. A. **82:**1257–1261. http://dx.doi.org/10.1073/pnas.82.4.1257.
26. **Henriksen S, Tylden GD, Dumoulin A, Sharma BN, Hirsch HH, Rinaldo CH.** 2014. The human fetal glial cell line SVG p12 contains infectious BK polyomavirus (BKPyV). J. Virol. **88:**7556–7568. http://dx.doi.org/10.1128/JVI.00696-14.
27. **Dondorp AM, Fanello CI, Hendriksen IC, Gomes E, Seni A, Chhaganlal KD, Bojang K, Olaosebikan R, Anunobi N, Maitland K, Kivaya E, Agbenyega T, Nguah SB, Evans J, Gesase S, Kahabuka C, Mtove G, Nadjm B, Deen J, Mwanga-Amumpaire J, Nansumba M, Karema C, Umulisa N, Uwimana A, Mokuolu OA, Adedoyin OT, Johnson WB, Tshefu AK, Onyamboko MA, Sakulthaew T, Ngum WP, Silamut K, Stepniewska K, Woodrow CJ, Bethell D, Wills B, Oneko M, Peto TE, von Seidlein L, Day NP, White NJ, AQUAMAT Group.** 2010. Artesunate versus quinine in the treatment of severe falciparum malaria in African children (AQUAMAT): an open-label, randomised trial. Lancet **376:**1647–1657. http://dx.doi.org/10.1016/S0140-6736(10)61924-1.
28. **Romero MR, Efferth T, Serrano MA, Castaño B, Macias RI, Briz O, Marin JJ.** 2005. Effect of artemisinin/artesunate as inhibitors of hepatitis B virus production in an "*in vitro*" replicative system. Antiviral Res. **68:**75–83. http://dx.doi.org/10.1016/j.antiviral.2005.07.005.
29. **Auerochs S, Korn K, Marschall M.** 2011. A reporter system for Epstein-Barr virus (EBV) lytic replication: anti-EBV activity of the broad antiherpesviral drug artesunate. J. Virol. Methods **173:**334–339. http://dx.doi.org/10.1016/j.jviromet.2011.03.005.
30. **Romero MR, Serrano MA, Vallejo M, Efferth T, Alvarez M, Marin JJ.** 2006. Antiviral effect of artemisinin from *Artemisia annua* against a model member of the *Flaviviridae* family, the bovine viral diarrhoea virus (BVDV). Planta Med. **72:**1169–1174. http://dx.doi.org/10.1055/s-2006-947198.
31. **Milbradt J, Auerochs S, Korn K, Marschall M.** 2009. Sensitivity of human herpesvirus 6 and other human herpesviruses to the broad-spectrum antiinfective drug artesunate. J. Clin. Virol. **46:**24–28. http://dx.doi.org/10.1016/j.jcv.2009.05.017.
32. **Efferth T, Romero MR, Wolf DG, Stamminger T, Marin JJ, Marschall M.** 2008. The antiviral activities of artemisinin and artesunate. Clin. Infect. Dis. **47:**804–811. http://dx.doi.org/10.1086/591195.
33. **Efferth T, Marschall M, Wang X, Huong SM, Hauber I, Olbrich A, Kronschnabl M, Stamminger T, Huang ES.** 2002. Antiviral activity of artesunate towards wild-type, recombinant, and ganciclovir-resistant human cytomegaloviruses. J. Mol. Med. (Berl.) **80:**233–242. http://dx.doi.org/10.1007/s00109-001-0300-8.
34. **Shapira MY, Resnick IB, Chou S, Neumann AU, Lurain NS, Stamminger T, Caplan O, Saleh N, Efferth T, Marschall M, Wolf DG.** 2008. Artesunate as a potent antiviral agent in a patient with late drug-resistant cytomegalovirus infection after hematopoietic stem cell transplantation. Clin. Infect. Dis. **46:**1455–1457. http://dx.doi.org/10.1086/587106.
35. **Germi R, Mariette C, Alain S, Lupo J, Thiebaut A, Brion JP, Epaulard O, Saint Raymond C, Malvezzi P, Morand P.** 2014. Success and failure of artesunate treatment in five transplant recipients with disease caused by drug-resistant cytomegalovirus. Antiviral Res. **101:**57–61. http://dx.doi.org/10.1016/j.antiviral.2013.10.014.
36. **Hakacova N, Klingel K, Kandolf R, Engdahl E, Fogdell-Hahn A, Higgins T.** 2013. First therapeutic use of artesunate in treatment of human herpesvirus 6B myocarditis in a child. J. Clin. Virol. **57:**157–160. http://dx.doi.org/10.1016/j.jcv.2013.02.005.
37. **Wolf DG, Shimoni A, Resnick IB, Stamminger T, Neumann AU, Chou S, Efferth T, Caplan O, Rose J, Nagler A, Marschall M.** 2011. Human cytomegalovirus kinetics following institution of artesunate after hematopoietic stem cell transplantation. Antiviral Res. **90:**183–186. http://dx.doi.org/10.1016/j.antiviral.2011.03.184.
38. **Lau PK, Woods ML, Ratanjee SK, John GT.** 2011. Artesunate is ineffective in controlling valganciclovir-resistant cytomegalovirus infection. Clin. Infect. Dis. **52:**279. http://dx.doi.org/10.1093/cid/ciq050.
39. **Sharma BN, Marschall M, Henriksen S, Rinaldo CH.** 2014. Antiviral effects of artesunate on polyomavirus BK replication in primary human kidney cells. Antimicrob. Agents Chemother. **58:**279–289. http://dx.doi.org/10.1128/AAC.01800-13.
40. **McLaurin J, Trudel GC, Shaw IT, Antel JP, Cashman NR.** 1995. A human glial hybrid cell line differentially expressing genes subserving oligodendrocyte and astrocyte phenotype. J. Neurobiol. **26:**283–293. http://dx.doi.org/10.1002/neu.480260212.
41. **Padgett BL, Walker DL, ZuRhein GM, Hodach AE, Chou SM.** 1976. JC papovavirus in progressive multifocal leukoencephalopathy. J. Infect. Dis. **133:**686–690. http://dx.doi.org/10.1093/infdis/133.6.686.
42. **Schweighardt B, Shieh JT, Atwood WJ.** 2001. CD4/CXCR4-independent infection of human astrocytes by a T-tropic strain of HIV-1. J. Neurovirol. **7:**155–162. http://dx.doi.org/10.1080/13550280152058816.
43. **Drachenberg CB, Hirsch HH, Papadimitriou JC, Gosert R, Wali RK, Munivenkatappa R, Nogueira J, Cangro CB, Haririan A, Mendley S, Ramos E.** 2007. Polyomavirus BK versus JC replication and nephropathy

in renal transplant recipients: a prospective evaluation. Transplantation **84:**323–330. http://dx.doi.org/10.1097/01.tp.0000269706.59977.a5.
44. **Hey AW, Johnsen JI, Johansen B, Traavik T.** 1994. A two fusion partner system for raising antibodies against small immunogens expressed in bacteria. J. Immunol. Methods **173:**149–156. http://dx.doi.org/10.1016/0022-1759(94)90294-1.
45. **Rinaldo CH, Gosert R, Bernhoff E, Finstad S, Hirsch HH.** 2010. 1-*O*-Hexadecyloxypropyl cidofovir (CMX001) effectively inhibits polyomavirus BK replication in primary human renal tubular epithelial cells. Antimicrob. Agents Chemother. **54:**4714–4722. http://dx.doi.org/10.1128/AAC.00974-10.
46. **Sharma BN, Li R, Bernhoff E, Gutteberg TJ, Rinaldo CH.** 2011. Fluoroquinolones inhibit human polyomavirus BK (BKV) replication in primary human kidney cells. Antiviral Res. **92:**115–123. http://dx.doi.org/10.1016/j.antiviral.2011.07.012.
47. **Schowalter RM, Buck CB.** 2013. The Merkel cell polyomavirus minor capsid protein. PLoS Pathog. **9:**e1003558. http://dx.doi.org/10.1371/journal.ppat.1003558.
48. **Mázló M, Tariska I.** 1982. Are astrocytes infected in progressive multifocal leukoencephalopathy (PML)? Acta Neuropathol. **56:**45–51. http://dx.doi.org/10.1007/BF00691181.
49. **Lööv C, Hillered L, Ebendal T, Erlandsson A.** 2012. Engulfing astrocytes protect neurons from contact-induced apoptosis following injury. PLoS One **7:**e33090. http://dx.doi.org/10.1371/journal.pone.0033090.
50. **Chou S, Marousek G, Auerochs S, Stamminger T, Milbradt J, Marschall M.** 2011. The unique antiviral activity of artesunate is broadly effective against human cytomegaloviruses including therapy-resistant mutants. Antiviral Res. **92:**364–368. http://dx.doi.org/10.1016/j.antiviral.2011.07.018.
51. **Efferth T, Kaina B.** 2010. Toxicity of the antimalarial artemisinin and its dervatives. Crit. Rev. Toxicol. **40:**405–421. http://dx.doi.org/10.3109/10408441003610571.
52. **Flobinus A, Taudon N, Desbordes M, Labrosse B, Simon F, Mazeron MC, Schnepf N.** 2014. Stability and antiviral activity against human cytomegalovirus of artemisinin derivatives. J. Antimicrob. Chemother. **69:**34–40. http://dx.doi.org/10.1093/jac/dkt346.
53. **Lynch KJ, Frisque RJ.** 1990. Identification of critical elements within the JC virus DNA replication origin. J. Virol. **64:**5812–5822.
54. **Jiang Z, Chai J, Chuang HH, Li S, Wang T, Cheng Y, Chen W, Zhou D.** 2012. Artesunate induces G_0/G_1 cell cycle arrest and iron-mediated mitochondrial apoptosis in A431 human epidermoid carcinoma cells. Anticancer Drugs **23:**606–613. http://dx.doi.org/10.1097/CAD.0b013e328350e8ac.
55. **Li S, Xue F, Cheng Z, Yang X, Wang S, Geng F, Pan L.** 2009. Effect of artesunate on inhibiting proliferation and inducing apoptosis of SP2/0 myeloma cells through affecting NFkappaB p65. Int. J. Hematol. **90:**513–521. http://dx.doi.org/10.1007/s12185-009-0409-z.
56. **Xu Q, Li ZX, Peng HQ, Sun ZW, Cheng RL, Ye ZM, Li WX.** 2011. Artesunate inhibits growth and induces apoptosis in human osteosarcoma HOS cell line *in vitro* and *in vivo*. J. Zhejiang Univ. Sci. B **12:**247–255. http://dx.doi.org/10.1631/jzus.B1000373.
57. **Sullivan CS, Pipas JM.** 2002. T antigens of simian virus 40: molecular chaperones for viral replication and tumorigenesis. Microbiol. Mol. Biol. Rev. **66:**179–202. http://dx.doi.org/10.1128/MMBR.66.2.179-202.2002.
58. **Heredero-Bermejo I, Copa-Patiño JL, Soliveri J, Gómez R, de la Mata FJ, Pérez-Serrano J.** 2013. *In vitro* comparative assessment of different viability assays in *Acanthamoeba castellanii* and *Acanthamoeba polyphaga* trophozoites. Parasitol. Res. **112:**4087–4095. http://dx.doi.org/10.1007/s00436-013-3599-5.
59. **Manning L, Laman M, Page-Sharp M, Salman S, Hwaiwhanje I, Morep N, Siba P, Mueller I, Karunajeewa HA, Davis TM.** 2011. Meningeal inflammation increases artemether concentrations in cerebrospinal fluid in Papua New Guinean children treated with intramuscular artemether. Antimicrob. Agents Chemother. **55:**5027–5033. http://dx.doi.org/10.1128/AAC.00375-11.
60. **Morris CA, Duparc S, Borghini-Fuhrer I, Jung D, Shin CS, Fleckenstein L.** 2011. Review of the clinical pharmacokinetics of artesunate and its active metabolite dihydroartemisinin following intravenous, intramuscular, oral or rectal administration. Malar. J. **10:**263. http://dx.doi.org/10.1186/1475-2875-10-263.
61. **Li Q, Cantilena LR, Leary KJ, Saviolakis GA, Miller RS, Melendez V, Weina PJ.** 2009. Pharmacokinetic profiles of artesunate after single intravenous doses at 0.5, 1, 2, 4, and 8 mg/kg in healthy volunteers: a phase I study. Am. J. Trop. Med. Hyg. **81:**615–621. http://dx.doi.org/10.4269/ajtmh.2009.09-0150.
62. **Miller RS, Li Q, Cantilena LR, Leary KJ, Saviolakis GA, Melendez V, Smith B, Weina PJ.** 2012. Pharmacokinetic profiles of artesunate following multiple intravenous doses of 2, 4, and 8 mg/kg in healthy volunteers: phase 1b study. Malar. J. **11:**255. http://dx.doi.org/10.1186/1475-2875-11-255.
63. **Davis TM, Binh TQ, Ilett KF, Batty KT, Phuöng HL, Chiswell GM, Phuong VDB, Agus C.** 2003. Penetration of dihydroartemisinin into cerebrospinal fluid after administration of intravenous artesunate in severe falciparum malaria. Antimicrob. Agents Chemother. **47:**368–370. http://dx.doi.org/10.1128/AAC.47.1.368-370.2003.
64. **Kearney BP, Aweeka FT.** 1999. The penetration of anti-infectives into the central nervous system. Neurol. Clin. **17:**883–900. http://dx.doi.org/10.1016/S0733-8619(05)70171-7.
65. **Schnepf N, Corvo J, Pors MJ, Mazeron MC.** 2011. Antiviral activity of ganciclovir and artesunate towards human cytomegalovirus in astrocytoma cells. Antiviral Res. **89:**186–188. http://dx.doi.org/10.1016/j.antiviral.2010.12.002.
66. **Bethell D, Se Y, Lon C, Tyner S, Saunders D, Sriwichai S, Darapiseth S, Teja-Isavadharm P, Khemawoot P, Schaecher K, Ruttvisutinunt W, Lin J, Kuntawungin W, Gosi P, Timmermans A, Smith B, Socheat D, Fukuda MM.** 2011. Artesunate dose escalation for the treatment of uncomplicated malaria in a region of reported artemisinin resistance: a randomized clinical trial. PLoS One **6:**e19283. http://dx.doi.org/10.1371/journal.pone.0019283.